JACS
JOURNAL OF THE AMERICAN CHEMICAL SOCIETY

Communication

pubs.acs.org/JACS

Isotope Effects Reveal the Mechanism of Enamine Formation in L-Proline-Catalyzed α-Amination of Aldehydes

Melissa A. Ashley,[†] Jennifer S. Hirschi,[†] Joseph A. Izzo, and Mathew J. Vetticatt*

Department of Chemistry, Binghamton University, Binghamton, New York 13902, United States

Supporting Information

ABSTRACT: The mechanism of L-proline-catalyzed α-amination of 3-phenylpropionaldehyde was studied using a combination of experimental kinetic isotope effects (KIEs) and theoretical calculations. Observation of a significant carbonyl ^{13}C KIE and a large primary α-deuterium KIE support rate-determining enamine formation. Theoretical predictions of KIEs exclude the widely accepted mechanism of enamine formation via intramolecular deprotonation of an iminium carboxylate intermediate. An E2 elimination mechanism catalyzed by a bifunctional base that directly forms an N-protonated enamine species from an oxazolidinone intermediate accounts for the experimental KIEs. These findings provide the first experimental picture of the transition-state geometry of enamine formation and clarify the role of oxazolidinones as nonparasitic intermediates in proline catalysis.

The L-proline-catalyzed α-functionalization of aldehydes via enamine catalysis has led to a number of powerful asymmetric transformations.[1] A single transition-state model—the Houk–List (H–L) model—provides a general rationale for the observed enantioselectivity in these reactions (Figure 1).[2] Central to this model is the *anti*-enamine carboxylic acid intermediate **8**, which serves as both an enolate equivalent and a Brønsted acid activator of the electrophile, via proton transfer from the carboxylic acid moiety, at the stereodetermining transition state **TS4** (Figure 1B). It is generally assumed that **8** is formed from **7** by an intramolecular deprotonation mechanism via **TS3**. Oxazolidinone intermediates such as **11** and **13** are considered off-cycle parasitic species within the H–L model.[3]

Seebach and Eschenmoser have proposed an alternate pathway (the S–E model) based on the observation of **11** and **13** by ^1H NMR spectroscopy.[4] The key intermediate in the S–E pathway for enamine catalysis is not **8** but *syn*-enamine carboxylate **12**. Formation of **12** occurs via E2 elimination from **11**. The electrophile-induced γ-lactonization of **12** to oxazolidinone **13** via **TS9** (Figure 1B) is the key stereodetermining event in this pathway. An NMR study by Gschwind and co-workers[5] supported a third mechanistic pathway: direct conversion of **11** to **8** (**TS-Gschwind**) without the intermediacy of **7**. The Gschwind model combines key features of the H–L and S–E mechanisms: an apparent E2 elimination from **11** (S–E proposal) results in the formation of H–L intermediate **8**, and **TS4** (H–L proposal) is the stereodetermining event in the catalytic cycle.

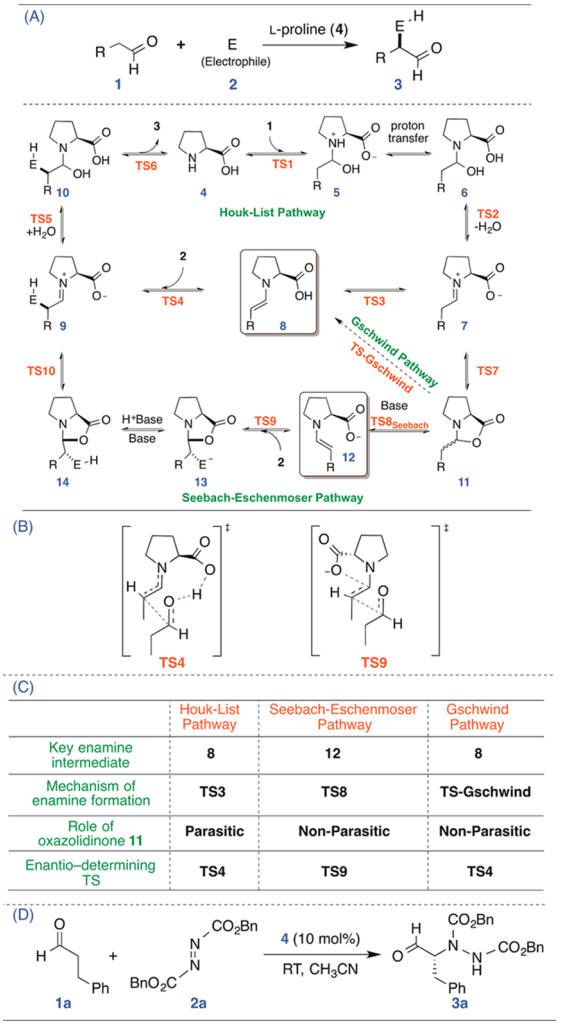

Figure 1. (A) Mechanistic models for enamine catalysis by L-proline show the three proposed pathways for enamine formation. (B) Houk–List (**TS4**) and Seebach–Eschenmoser (**TS9**) transition-state models for the origin of enantioselectivity in the L-proline-catalyzed aldol reaction. (C) Distinguishing features of the three mechanistic models for enamine catalysis. (D) Prototypical reaction proceeding via rate-determining enamine formation.

The three mechanisms discussed (Figure 1A) are different with respect to (a) the mechanism of enamine formation, (b) the

Received: October 17, 2015
Published: January 15, 2016

ACS Publications © 2016 American Chemical Society

DOI: 10.1021/jacs.5b10876
J. Am. Chem. Soc. 2016, 138, 1756–1759

role of oxazolidinone intermediate **11**, and (c) the nature of the enantioselectivity-determining step (Figure 1C). While there is little debate that **TS4** (H−L model) is the stereodetermining transition state,[6] the exact mechanism of enamine formation and the role of **11** in proline catalysis are not firmly established. Here we report the results of a combined experimental and theoretical ^{13}C and ^{2}H kinetic isotope effect (KIE) study that provides the first experimental insights into the transition-state geometry for enamine formation and clarifies the role of oxazolidinone intermediates in proline catalysis.

The mechanism of L-proline-catalyzed α-amination of aldehydes (Figure 1D)[7] has been investigated using experimental[8] and computational[9] methods. Kinetic studies by Blackmond revealed that the reaction (a) is zero-order in electrophile, (b) exhibits asymmetric amplification, and (c) is autocatalytic. Enamine formation has been implicated as the rate-determining step in the catalytic cycle. This reaction was therefore chosen for determination of ^{13}C and ^{2}H KIEs as a direct probe of the mechanism of enamine formation in catalysis by proline.

Experimental KIEs. Experimental ^{13}C KIEs for **1a** were determined from analysis of the starting material using NMR methodology at natural abundance.[10] Two separate reactions of **1a** and **2a** were taken to 84 ± 2% and 77 ± 2% conversion of **1a**. Unreacted **1a** was reisolated from the reaction mixture, and the ^{13}C isotopic composition was compared to that of samples of **1a** not subjected to the reaction conditions.[11] From the changes in relative isotopic composition and the fractional conversion, the ^{13}C KIEs were determined. Additionally, α-deuterium KIEs ($k_{H\text{-}2}/k_{D\text{-}2}$) were measured from two independent reactions of a 4:1 α-H_2-**1a**:α-D_2-**1a** mixture taken to 48 ± 2% and 47 ± 2% conversion of α-H_2-**1a** using ^{2}H NMR analysis (of $NaBD_4$-reduced reaction mixtures) to accurately determine the enhancement of deuterium content in the unreacted starting material.[11] The experimentally measured ^{13}C and ^{2}H KIEs from the four independent experiments are shown in Figure 2.

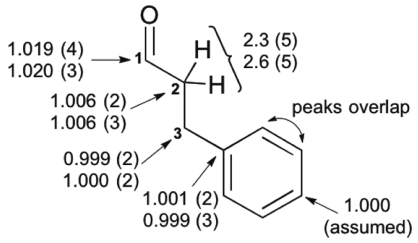

Figure 2. Experimental KIEs for the L-proline-catalyzed reaction of **1a** with **2a**. The two sets of ^{13}C KIEs and two sets of ^{2}H KIEs represent independent experiments with six measurements per experiment. For each measurement, the number in parentheses shows the uncertainty in the last digit.

Qualitative interpretation of experimental KIEs. The observation of a significant carbonyl (C1) ^{13}C KIE and a large primary (1°) α-deuterium KIE ($k_{H\text{-}2}/k_{D\text{-}2}$) is indicative of a rate-determining step involving α-deprotonation concomitant with bonding changes at C1. The small yet nonunity KIE on the α-carbon (C2) suggests that C2 is not completely rehybridized during the proton transfer event. The experimental KIEs are qualitatively consistent with a mechanism involving rate-determining E2 elimination; however, a quantitative interpretation is deferred until all of the possible transition structures in the various models (Figure 1A) are ruled out by a comparison of the predicted KIEs with the experimental values.

Theoretical studies. To aid in this quantitative interpretation of the experimental KIEs, transition structures for all of the steps in Figure 1A were computed using the B3LYP-GD3 method[12,13] with the 6-31+G** basis set and the PCM solvent model[14] for acetonitrile. This method adequately describes the energetics and predicts the KIEs in other proline-catalyzed reactions.[15] The ^{13}C and ^{2}H KIEs were computed from the scaled vibrational frequencies of the respective transition structures using the program ISOEFF98.[16,17] A Wigner tunneling correction was applied to all of the predicted KIEs.[18]

Table 1. Comparison of Experimental and Predicted KIEs for all of the Transition Structures in Figure 1 Not Involved in Enamine Formation

Predicted KIEs	C1	C2	C3	$k_{1\text{-}\alpha\text{-}H2}/k_{1\text{-}\alpha\text{-}D2}$
TS1	1.025	1.001	1.005	0.8
TS2	1.024	0.994	1.000	0.8
TS4	1.004	1.018	1.001	1.0
TS5	1.027	0.985	1.000	0.6
TS6	1.020	0.988	0.999	0.6
TS7	1.026	1.002	1.000	0.9
TS9·H⁺	1.028	1.006	1.003	0.9
TS10	1.028	0.990	1.000	0.6
Experimental	1.019 (4) 1.020 (3)	1.006 (2) 1.006 (3)	0.999 (2) 1.000 (2)	2.3 (5) 2.6 (5)

KIEs for steps not involved in enamine formation. A comparison of the experimental and predicted KIEs for all of the transition structures in Figure 1A except for those involved in enamine formation (**TS3**, **TS8**, and **TS-Gschwind**) are shown in Table 1.[19] A key observation is the poor match between *all* of the experimental and predicted KIEs for **TS4** (the H−L TS). This confirms Blackmond's finding[8c] that **TS4** is not rate-determining. The predicted ^{13}C KIEs on C1 for the remaining transition structures (Table 1) are reasonably close to the experimental C1 KIE. However, the corresponding predicted α-^{2}H KIEs for these transition structures are inverse—an unsurprising observation considering that the α-carbon is either uninvolved or completely rehybridized in all of these structures. Thus, the experimental 1° α-deuterium KIE excludes all of the structures in Table 1 as the rate-determining step in catalysis.

Transition structures and KIEs for enamine formation. The next step was to explore all of the possible transition structures for

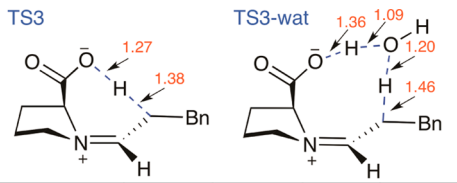

Predicted KIEs for TS3	C1	C2	C3	$k_{1\text{-}\alpha\text{-}H2}/k_{1\text{-}\alpha\text{-}D2}$
TS3	1.002	1.008	1.001	6.6
TS3-wat	1.002	1.007	1.002	5.6
Experimental	1.019 (4) 1.020 (3)	1.006 (2) 1.006 (3)	0.999 (2) 1.000 (2)	2.3 (5) 2.6 (5)

Figure 3. Lowest-energy transition structures for enamine formation via deprotonation of 7 and comparison of experimental and predicted KIEs.[19]

DOI: 10.1021/jacs.5b10876
J. Am. Chem. Soc. 2016, 138, 1756−1759

enamine formation and compare the KIE predictions for each structure to the experimental values. Intramolecular deprotonation of the α-proton of **7** by the carboxylate moiety (**TS3**) is the proposed mechanism of enamine formation in the H−L pathway. This mechanism, along with water-assisted conversion of **7** to **8** (**TS3-wat**), has previously been studied computationally (Figure 3).[6] While the predicted normal α-^{2}H KIEs for **TS3** and **TS3-wat** are in crude agreement with experiment, the near-unity predicted ^{13}C KIE on C1 is clearly inconsistent with experiment (Figure 3). *This result strongly rules against the widely accepted notion that iminium carboxylate 7 is a direct precursor to key enamine intermediate 8.*

Direct conversion of **11** to **12** (**TS8$_{Seebach}$**) or **11** to **8** (**TS-Gschwind**) occurs via an elimination mechanism involving α-deprotonation and C−O bond scission (Figure 4).[20] Seebach has proposed that an E2 elimination pathway[4]—represented by the diagonal in the More O'Ferrall−Jencks plot for this transformation (Figure 4)—could be initiated by a number of bases, including another molecule of **4**, **11**, or even the product **3a** (autocatalysis). We tried modeling **TS8$_{Seebach}$** (or **TS-Gschwind**) using these and other bases, but all attempts to locate an E2 elimination transition structure resulted in geometries with the C−O bond completely cleaved as the base deprotonated the α-proton. This corresponds to the second step in a stepwise E1 elimination mechanism proceeding via the zwitterionic intermediate **7** − unsurprising, considering that α-deprotonation is more likely to occur from **7** than from the less acidic **11**. The magnitude of the predicted α-deuterium KIE for **TS8$_{Seebach}$** depends on the extent of deprotonation, which is a function of the base employed for the particular calculation. However, the near-complete C−O bond cleavage in all of these structures leads to close-to-unity values for the predicted C1 KIE, an observation that is in clear disagreement with the ∼2% experimental measurement.[21]

The conversion of **11** to **12** favors a stepwise E1 elimination mechanism over a concerted E2 pathway due to stabilization of the carbocation intermediate by the lone pair of electrons on the pyrrolidine nitrogen. However, the experimental KIEs point toward a concerted pathway. Disengaging the nitrogen lone pair from the reaction coordinate for the elimination, by H-bonding or protonation, destabilizes the bottom left corner of Figure 4 and shifts **TS8$_{Seebach}$** toward an E2-type transition structure. On the basis of this reasoning, an alternate mechanism for the direct formation of an enamine intermediate from **11** is proposed (Figure 5). In this new transition structure **TS8′**, a bifunctional acid−base molecule protonates the pyrrolidine nitrogen while simultaneously deprotonating the α-proton of **11**. The initial product from **TS8′** is N-protonated *syn-* or *anti*-enamine carboxylate **12·H$^+$** which can re-enter the H−L pathway after a proton transfer to form **8** (Figure 5).

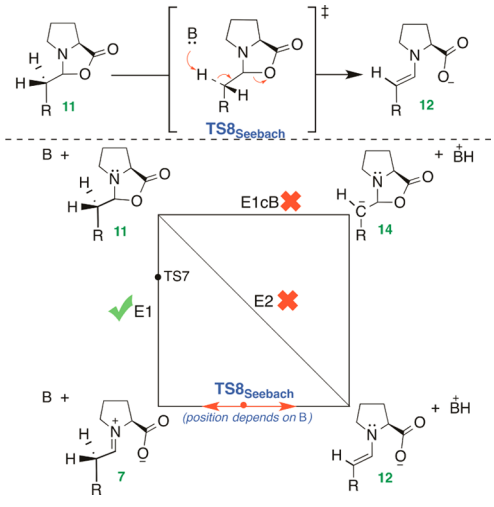

Figure 4. More O'Ferrall−Jencks plot summarizing the possible elimination pathways for the conversion of **11** to **12**. The bottom left corner of the plot corresponds to zwitterionic intermediate **7**, which facilitates an E1 elimination pathway.

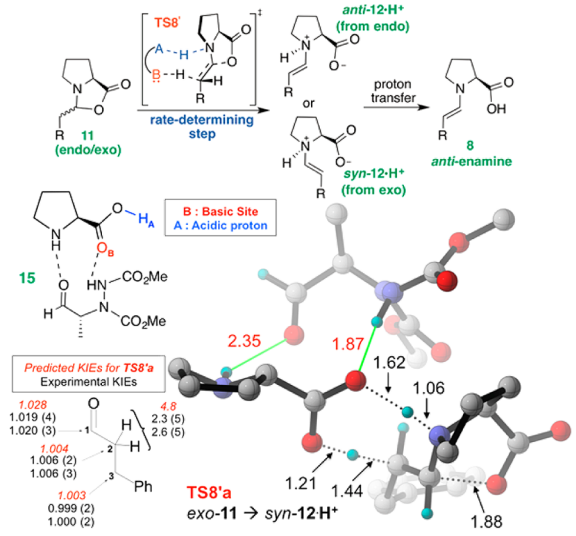

Figure 5. Transition structure **TS8′a** for an E2 elimination mechanism consistent with the experimental KIEs. Most of the hydrogens have been removed for clarity. Key bond-breaking/making (black) and H-bonding (red) distances (in Å) are shown along with the predicted KIEs.

Several bifunctional bases[22] were employed to model **TS8′**, and the best match of experimental and predicted KIEs was obtained when soluble product−proline H-bonded complex **15** was employed as the bifunctional base to effect the direct conversion of *exo*-**11** to *syn*-**12·H$^+$**. The key features of the resulting transition-state geometry **TS8′a**, along with a comparison of the experimental and predicted KIEs, are shown in Figure 5. Considering the complete mismatch between the experimental and theoretical KIEs for every transition structure modeled thus far (**TS1**−**10**), the predicted values for **TS8′a** provide the *best simultaneous* match to all three key experimental measurements, namely, the C1, C2, and α-deuterium KIEs. Finally, the calculated *E* + ZPE and free energy barriers for **TS8′a** are 14.1 and 28.0 kcal/mol, respectively, which are consistent with the facility of the reaction.[23] *These results strongly support E2 elimination from 11 as the most likely mechanism of enamine formation in proline catalysis.* We recognize that the predicted α-deuterium KIEs for **TS8′a** are high compared with the experimental values.[19] Uncertainty regarding the exact identity of the base that catalyzes **TS8′** possibly accounts for this discrepancy. This inconsistency could also arise from the known failure of calculations based on conventional transition-state theory (TST) to accurately describe structures with concomitant heavy- and light-atom motion.[24] A variational TST[25] treatment, for example, may give predictions that are closer to experiment, but the broad mechanistic picture that would emerge from such advanced calculations is expected to be identical to the conclusions presented herein.

DOI: 10.1021/jacs.5b10876
J. Am. Chem. Soc. 2016, 138, 1756−1759

Our proposal that **15** is likely the bifunctional base that catalyzes the rate-determining step (**TS8′**) is consistent with (a) Seebach's proposal[4] that base catalysis is the chemical origin of the autocatalysis observed in this reaction (i.e., that product formation accelerates the reaction by increasing the concentration of the base that catalyzes the rate-determining step) and (b) Blackmond's observation that the autocatalytic nature of this reaction is a result of "a catalytic cycle involving only soluble proline complexes or soluble proline adducts".[8a] After the original submission of this article, we were made aware of a new NMR study by Gschwind and co-workers probing the mechanism of enamine formation in the proline-catalyzed self-aldol reaction of 3-methylbutanal in dimethyl sulfoxide (DMSO).[26] This new study rescinds their original proposal (ref 5, **TS-Gschwind**) and supports the H−L pathway (**TS3**) as the most likely mechanism of enamine formation. This is in direct conflict with our results (vide supra) and led us to further question the conclusions presented herein.

We questioned whether our experimental KIEs could have resulted from multiple steps in the catalytic cycle being partially rate-determining; for example, a weighted average of the predicted KIEs of **TS2** and **TS3** could potentially account for our experimental KIEs. In order to probe this possibility experimentally, we determined the C1 KIEs using α-D_2-**1a** as the aldehyde. If **TS3** were indeed partially rate-determining, it would be expected that α-deuteriums would increase the barrier to **TS3** and make it "more rate-determining". This would result in a C1 KIE value closer to the predicted value for **TS3** (1.002; Figure 3). We conducted duplicate ^{13}C KIE experiments using α-D_2-**1a** and obtained C1 KIE values of 1.024(4) and 1.021(4)—virtually identical to our measurements using **1a**.[11] *This result confirms that our experimental KIEs originate from a single rate-determining step and reaffirms that **TS3** is not involved in the mechanism of enamine formation in our system.* The discrepancy between our study and ref 26 is most likely attributable to the choice of electrophile (**2a** vs 3-methylbutanal) and/or solvent (acetonitrile vs DMSO) for the respective reactions.

In conclusion, this work resolves the mechanism of enamine formation in the proline-catalyzed α-amination of aldehydes. Our data support a mechanism involving direct conversion of oxazolidinone **11** to N-protonated enamine **12**·H^+ via an E2 elimination initiated by a bifunctional base. Rapid proton transfer from **12**·H^+ presumably forms **8** followed by re-entry into the Houk−List pathway. These results confirm the role of oxazolidinone **11** as a key *nonparasitic* intermediate in the Houk−List catalytic cycle while invoking base catalysis as the possible origin of autocatalysis observed in this reaction.

■ ASSOCIATED CONTENT

Supporting Information

The Supporting Information is available free of charge on the ACS Publications website at DOI: 10.1021/jacs.5b10876.

Complete experimental and computational details and NMR data (PDF)

■ AUTHOR INFORMATION

Corresponding Author

*vetticatt@binghamton.edu

Author Contributions

†M.A.A. and J.S.H. contributed equally.

Notes

The authors declare no competing financial interest.

■ ACKNOWLEDGMENTS

M.J.V. acknowledges support from startup funding at Binghamton University from the SUNY Research Foundation and the National Science Foundation through XSEDE resources provided by the XSEDE Science Gateways Program.

■ REFERENCES

(1) *Science of Synthesis: Asymmetric Organocatalysis I*; List, B., Maruoka, K., Eds.; Thieme: Stuttgart, Germany, 2012.

(2) Bahmanyar, S.; Houk, K. N.; Martin, H. J.; List, B. *J. Am. Chem. Soc.* **2003**, *125*, 2475−2479.

(3) (a) List, B.; Hoang, L.; Martin, H. J. *Proc. Natl. Acad. Sci. U. S. A.* **2004**, *101*, 5839−5842. (b) Bock, D. A.; Lehmann, C. W.; List, B. *Proc. Natl. Acad. Sci. U. S. A.* **2010**, *107*, 20636−20641.

(4) Seebach, D.; Beck, A. K.; Badine, D. M.; Limbach, M.; Eschenmoser, A.; Treasurywala, A. M.; Hobi, R.; Prikoszovich, W.; Linder, B. *Helv. Chim. Acta* **2007**, *90*, 425−471.

(5) Schmid, M. B.; Zeitler, K.; Gschwind, R. M. *Angew. Chem., Int. Ed.* **2010**, *49*, 4997−5003.

(6) Sharma, A. K.; Sunoj, R. B. *Angew. Chem., Int. Ed.* **2010**, *49*, 6373−6377.

(7) List, B. *J. Am. Chem. Soc.* **2002**, *124*, 5656−5657.

(8) (a) Iwamura, H.; Wells, D. H.; Mathew, S. P.; Klussmann, M.; Armstrong, A.; Blackmond, D. G. *J. Am. Chem. Soc.* **2004**, *126*, 16312−16313. (b) Iwamura, H.; Mathew, S. P.; Blackmond, D. G. *J. Am. Chem. Soc.* **2004**, *126*, 11770−11771. (c) Mathew, S. P.; Klussmann, M.; Iwamura, H.; Wells, D. H., Jr.; Armstrong, A.; Blackmond, D. G. *Chem. Commun.* **2006**, 4291−4293.

(9) Sharma, A. K.; Sunoj, R. B. *Chem. Commun.* **2011**, *47*, 5759−5761.

(10) Singleton, D. A.; Thomas, A. A. *J. Am. Chem. Soc.* **1995**, *117*, 9357−9358.

(11) See the Supporting Information (SI) for a detailed description of the experiments involved in the determination of KIEs.

(12) Becke, A. D. *J. Chem. Phys.* **1993**, *98*, 5648−5652.

(13) Grimme, S.; Antony, J.; Ehrlich, S.; Krieg, H. *J. Chem. Phys.* **2010**, *132*, 154104.

(14) Tomasi, J.; Mennucci, B.; Cammi, R. *Chem. Rev.* **2005**, *105*, 2999−3093.

(15) Zhu, H.; Clemente, F. R.; Houk, K. N.; Meyer, M. P. *J. Am. Chem. Soc.* **2009**, *131*, 1632−1633.

(16) Anisimov, V.; Paneth, P. *J. Math. Chem.* **1999**, *26*, 75.

(17) The frequencies were scaled by 0.9614. See: Scott, A. P.; Radom, L. *J. Phys. Chem.* **1996**, *100*, 16502.

(18) Bell, R. P. *The Tunnel Effect in Chemistry*; Chapman & Hall: London, 1980.

(19) These transition structures and predicted KIEs were calculated using multiple DFT methods (see the SI for geometries and full details).

(20) To model **TS-Gschwind**, a Brønsted acid (AcOH) was added to **TS8** to stabilize the incipient carboxylate moiety.

(21) See the SI for detailed discussion.

(22) Since the exact identity of the bifunctional base that catalyzes **TS8′** is unknown, transition structures corresponding to **TS8′** were located using a variety of bifunctional bases (see the SI for full details).

(23) See the SI for energy barriers for **TS8′a** calculated using several DFT methods. For an important discussion of the interpretation of calculated free energy barriers, see: Plata, R. E.; Singleton, D. A. *J. Am. Chem. Soc.* **2015**, *137*, 3811−3826.

(24) Vetticatt, M. J. Ph.D. Dissertation, Texas A&M University, College Station, TX, 2009.

(25) Truhlar, D. G.; Garrett, B. C. *Acc. Chem. Res.* **1980**, *13*, 440−448.

(26) Haindl, M. H.; Hioe, J.; Gschwind, R. M. *J. Am. Chem. Soc.* **2015**, *137*, 12835−12842.

DOI: 10.1021/jacs.5b10876
J. Am. Chem. Soc. 2016, 138, 1756−1759